



HAL
open science

Actively lubricated hybrid journal bearings based on magnetic fluids for high-precision spindles of machine tools

Luis Norberto Lopez de Lacalle, Harkaitz Urreta, Gorka Aguirre, Pavel Kuzhir, Luis Norberto López de Lacalle

► **To cite this version:**

Luis Norberto Lopez de Lacalle, Harkaitz Urreta, Gorka Aguirre, Pavel Kuzhir, Luis Norberto López de Lacalle. Actively lubricated hybrid journal bearings based on magnetic fluids for high-precision spindles of machine tools. *Journal of Intelligent Material Systems and Structures*, 2019, 30 (15), pp.2257-2271. 10.1177/1045389X19862358. hal-02426104

HAL Id: hal-02426104

<https://hal.science/hal-02426104>

Submitted on 1 Jan 2020

HAL is a multi-disciplinary open access archive for the deposit and dissemination of scientific research documents, whether they are published or not. The documents may come from teaching and research institutions in France or abroad, or from public or private research centers.

L'archive ouverte pluridisciplinaire **HAL**, est destinée au dépôt et à la diffusion de documents scientifiques de niveau recherche, publiés ou non, émanant des établissements d'enseignement et de recherche français ou étrangers, des laboratoires publics ou privés.

Actively lubricated hybrid journal bearings based on magnetic fluids for high precision spindles of machine tools

Harkaitz Urreta^{1*}, Gorka Aguirre¹, Pavel Kuzhir², Luis Norberto Lopez de Lacalle³

1 IK4-IDEKO, Arriaga 2, E-20870 Elgoibar, Spain

2 University Côte d'Azur, CNRS UMR 7010 Inst. of Physics of Nice, Parc Valrose 06100 Nice, France

3 EHU-UPV Dept. Mechanical Engineering, Alameda Urquijo S/N, E-48013 Bilbao, Spain

* Corresponding author hurreta@ideko.es; Tel: +34943748000 ; Fax: +34943743804

Abstract

The research work reported in this paper is focused on the use of magnetic fluids as active lubricant for improving the performance of hybrid journal bearings, with application to high precision machine tools. Prototype design was optimized following numerical computation of Reynolds equation and computational fluid dynamics (CFD) calculations, in both cases with Herschel-Buckley model for the magnetorheological fluid. This fluid (LORD Corp. MRF 122-2ED) was experimentally characterized in detail. The improvement of the hydrodynamic effect in journal bearings was demonstrated with 50% higher load capacity and stiffness, mainly at half of shaft eccentricity $0.4 < \varepsilon < 0.7$. Active hydrostatic lubrication achieved quasi-infinite stiffness

1
2
3 within working limits (load and speed), at low frequencies. For high dynamic response
4 the active lubrication based on magnetorheological valves did not show good response.
5 The feasibility of using magnetic fluids for developing high performance machine tool
6 spindles and the validity of the simulation models was demonstrated experimentally.
7
8
9

10 11 12 **Keywords**

13
14
15 Magnetorheological fluid, MR valves, active bearing, CFD, machine tool, spindle.
16
17
18
19
20
21
22
23
24
25
26
27
28
29
30
31
32
33
34
35
36
37
38
39
40
41
42
43
44
45
46
47
48
49
50
51
52
53
54
55
56
57
58
59
60

For Peer Review

Nomenclature and main variables

| | | | | | |
|---------------------------------|--|------------------------|--|--|----------------------|
| b | Recess width | [m] | S | Stiffness | [N/m] |
| B | Magnetic flux density | [T] | t | Time | [s] |
| C | Radial clearance | [m] | T | Temperature | [°C] |
| F | Force | [N] | W | Load capacity | [N] |
| F_f | Friction force | [N] | x,y,z | Linear coordinates | [-] |
| h | Film thickness | [m] | r,θ,z | Cylind. coordinates | [-] |
| H | Magnetic field strength | [A/m] | u,v,w | Fluid velocity | [m/s] |
| l | Recess length | [m] | $\dot{\gamma}$ | Shear rate | [1/s] |
| L | Bearing length | [m] | θ | Angular coordinate | [°] |
| n | Number of pockets | [-] | ρ | Density | [kg/m ³] |
| p | Pressure distribution | [Pa] | σ | Stress | [Pa] |
| P_r | Recess pressure | [Pa] | τ | Shear stress | [Pa] |
| P_p | Pumping pressure | [Pa] | μ | Dynamic viscosity | [Pa·s] |
| Q | Flowrate | [m ³ /s] | ν | Kinematic viscosity | [m ² /s] |
| R | Radius | [m] | φ | Attitude angle | [°] |
| R_a | Shaft radius | [m] | ψ | Angular abscissa | [°] |
| R_c | Bearing radius | [m] | Ω | Angular speed | [1/s] |
| R_h | Hydraulic resistance | [Pa·s/m ³] | | | |
| R_o | Hydraulic resist. bearing | [Pa·s/m ³] | | | |
| R_i | Hydraulic resist. restrictor | [Pa·s/m ³] | | | |
| $\beta = \frac{1}{1 + R_i/R_o}$ | Hydraulic resistance ratio | | $\lambda = \frac{L}{2R}$ | Length to diameter ratio | |
| $\varepsilon = \frac{e}{R}$ | Relative eccentricity | | $\tau_0^* = \frac{\tau_0 C}{\mu_0 R \omega}$ | Dimensionless yield stress | |
| $\Delta X = \frac{\Delta x}{R}$ | Dimensionless element size in tangential direction | | $H = \frac{h}{C}$ | Dimensionless gap size | |
| $\Delta Y = \frac{\Delta h}{h}$ | Dimensionless element size in radial direction | | $P = \frac{p(C/R)^2}{\mu \omega}$ | Dimensionless pressure | |
| $\Delta Z = \frac{\Delta z}{L}$ | Dimensionless element size in axial direction | | $\frac{dP}{dX} = \frac{dp}{dx} \frac{(C/R)^2}{\mu \omega}$ | Dimensionless pressure gradient tangential | |
| $u = \frac{v_x}{\omega R}$ | Dimensionless velocity in tangential direction | | $\frac{dP}{dZ} = \frac{dp}{dz} \frac{(C/R)^2}{\mu \omega}$ | Dimensionless pressure gradient axial | |
| $w = \frac{v_z}{\omega R}$ | Dimensionless velocity in axial direction | | | | |

INTRODUCTION

The introduction to this research work has three sections, 1) a brief introduction to classic lubricated bearings with hydrostatic and hydrodynamic lubrication, 2) active bearings and 3) active hybrid journal bearings with magnetic fluid.

Hydrostatic and hydrodynamic lubrication bearings

Pressurized lubricated bearings, commonly known as hydrostatic or hydrodynamic bearings, are quite widely used and known by manufacturers of high-precision machine tools. Most influencing authors in the machine tool building field, for instance M. Weck (Weck, 1984), agree that between the available technologies for guiding systems, namely sliding, rolling and pressurized lubricant technologies, the latter offers better properties, considering resolution, damping and smoothness in the movement. Lubricated bearings can work in either hydrostatic or hydrodynamic regime, in function of the boundary conditions, i.e.: external oil pressurization, geometry of the bearing, fluid viscosity and applied load.

Hydrodynamic bearings, where pressure is generated by relative motion between the bearing surfaces (Frêne et al., 1997), are suitable for applications where working conditions are quite stationary. Thus, with a proper design of the bearing, a stable and safe pressurized oil thin film can be achieved between the moving parts, the shaft and the bearing, avoiding any contact, friction and therefore wear. The pressure in the bearing follows the classic equation in thin fluid films proposed by Osborne Reynolds (Reynolds, 1886). The main hydrodynamic bearing drawback are the starting and deceleration stages, where fluid velocity is so low that lubricant film cannot support the load, leading to contact, friction and wear of surfaces.

To avoid contact and wear whatever is relative movement speed, hydrostatic lubrication (Bassani and Piccigallo, 1992) is the proper solution. In this case, lubricant

fluid pressure is provided by an external hydraulic pump, which ensures a fully developed thin lubricant film between bearing and shaft. The bearing behaviour is strongly dependent on the selection of compensation valves, commonly known as *restrictors*. Restrictors determine fundamental mechanical properties of the bearing, like stiffness and force. With increasing shaft speed, hydrodynamic pressure appears in the hydrostatic bearings, as described by Reynolds equation. Hydrostatic bearings can thus, in function of the geometry, oil viscosity and operational conditions, become in a “hybrid bearing” with mixed hydrodynamic and hydrostatic lubrication regime. Figure 1 scheme shows the bearing hydrodynamic pressure governed by Reynolds equation (1).

[insert figure 1]

Figure 1 Hydrodynamic pressure in journal bearings.

$$\frac{\partial}{\partial x} \left(\frac{\rho h^3}{\mu} \frac{\partial p}{\partial x} \right) + \frac{\partial}{\partial z} \left(\frac{\rho h^3}{\mu} \frac{\partial p}{\partial z} \right) = 6\rho(U_1 + U_2) \frac{\partial h}{\partial x} + 6\rho h \frac{\partial}{\partial x} (U_1 - U_2) + 12\rho V + 12\dot{\rho} h \quad (1)$$

Figure 2 shows the implementation of hydrostatic lubrication ruled by the basic equations (2).

[insert figure 2]

Figure 2 Hybrid journal bearing and hydraulic circuit

$$P_r = \beta \cdot P_p = \frac{1}{1 + R_i/R_o} \cdot P_p \quad W = \int_{-L}^{+L} \int_{-\pi}^{+\pi} p \cdot dA \quad S = \frac{dW}{d\varepsilon} \quad (2)$$

The improvement of the performance of journal bearing with hybrid lubrication by means of active magnetic fluids will be discussed in this paper.

Active bearings for smart systems

Following Reynolds and hydrostatic lubrication basic equations, see Eqs. (1) and (2), an active lubricated bearing can be achieved by the modification of bearing geometry, fluid viscosity and/or restrictor hydraulic resistance, the latter in the case of hydrostatic bearings.

1
2
3
4
5
6
7
8
9
10
11
12
13
14
15
16
17
18
19
20
21
22
23
24
25
26
27
28
29
30
31
32
33
34
35
36
37
38
39
40
41
42
43
44
45
46
47
48
49
50
51
52
53
54
55
56
57
58
59
60

Geometry change is a very complex option due the requirement of a mechanism to produce micrometric deformation with as large as possible stiffness. This solution has been explored with active air bearings by including flexible structures driven by piezo actuators (Aguirre et al., 2010; Morosi and Santos, 2011; Shamoto et al., 2006), but they are not transposable to high pressure hybrid journal bearings. Working with oil lubricated bearings, different approaches can be found in bibliography for pure hydrodynamic cases, e.g. closed loop control in oil feeding (Albers et al., 2011) to improve the energy efficiency of guiding, and in the particular case of tilting pads hydrodynamic bearings (Deckler, 2004; Nicoletti and Santos, 2003; Sun and Krodkiwski, 1999), the lubrication conditions and tilting angle of pads were modified by hydraulic or electromechanical actuators.

Regarding active bearings with hydrostatic lubrication, therefore with active restrictors (Jordan, 2000), some other research works aimed at a) the improvement of hybrid bearings with servo-valves (Santos and Watanabe, 2006), b) the study of active lubrication in complex multibody simulation (Estupiñan and Santos, 2009), and c) special considerations required for flexible rotors typical of energy generation machinery (Nicoletti and Santos, 2008). But a common characteristic in all those works was either the use of complex mechanisms for the bearing, or precise servo-valves for lubricant feeding.

Active hybrid lubricated bearings with magnetic fluids

A second research strand about actively lubricated bearings was focused on the use of fluids with rheological response under external exciting fields: electro-rheological fluids and magnetic fluids.

Electrorheological fluids change their rheology under electric field, increasing the shear stress proportionally to the field. Some research works developed active bearings (hydrodynamic and hydrostatic) using this kind of fluid as lubricant, e.g. in high-speed journal bearings to control stiffness and stability (G. Nikolakopoulos and Papadopoulos, 1998), describing the theoretical behaviour of journal bearings lubricated with active

1
2
3 fluids (Peng and Zhu, 2005), and studying the use of electrorheological fluids for active
4 hydrostatic bearings (Bouزيدane et al., 2008). In all those cases the high voltage (in the
5 range of 1-10kV) electric field required achieve a high enough electrorheological effect
6 was reported as a serious drawback for industrial implementation.
7
8
9

10
11 Regarding magnetic fluids, two main groups can be noted: ferrofluids and
12 magnetorheological fluids, hereinafter MRF. All magnetic fluids are composed by a
13 carrier fluid (lubricant oil in this case), additives to improve tribology and fluid stability,
14 and magnetic particles, which in function of their size (nanometric or micrometric) define
15 their behaviour. Ferrofluids contain stabilized nanometric particles (5-12nm diameter),
16 where due to their size and energy balance (gravity < particle's thermal energy) the
17 colloidal suspension is stable in time. Those particles are usually formed by iron or cobalt
18 oxides, covered with surfactants (oleic acid-like, the most extended) to avoid aggregation
19 and final settling of particles. The most relevant reference is the compilation book by S.
20 Odenbach (Odenbach, 2002), in which fluids synthesis, rheological characterization and
21 several applications are discussed.
22
23
24
25
26
27
28
29
30
31

32 The MRF are similar to ferrofluids but magnetic particles are in the range of
33 micrometres, from 1-10 μ m, mainly made of carbonyl iron powder, hereinafter CIP. They
34 are strongly unstable, as a matter of fact in few minutes the particles are settled on the
35 tank bottom. To avoid agglomeration and to have a quick restoration of homogeneous
36 MRF, the fluid may include several additives, and in a few removing or pumping cycles
37 the fluid can get its original behaviour.
38
39
40
41
42
43

44 The application of magnetic fluids in lubricated bearings was studied in some previous
45 works with two main approaches: Hydrodynamic and hydrostatic. In the case of
46 hydrodynamic bearings the magnetic field is applied directly into the bearing, modifying
47 the rheology of the fluid in the pressurized thin film. The hydrostatic lubrication is based
48 in the active restrictor that feed the bearing with controlled flowrate and pressures.
49
50
51
52
53

54 Starting with hydrodynamic lubrication, notorious changes in the Stribeck curve were
55 observed experimentally with the use of ferrofluids (Spur and Patzwald, 1998). The use
56
57
58
59
60

1
2
3 of ferrofluids in lubricated bearings design was also tackled by Osman et al., (T. A.
4 Osman et al., 2001), focusing on the static and dynamic response (T.A. Osman et al.,
5 2001), and the misalignment effect between shaft and bearing (Osman, 2001). A deeper
6 approach about magnetic fluids as lubricants was developed by (Uhlmann et al., 2002)
7 with a later application to journal bearings (Uhlmann and Bayat, 2003). More recent
8 works in this matter (Kuzhir et al. 2011; Hsu et al. 2013), aimed at the study of the free
9 boundary laws and the effect of surface roughness.
10
11

12
13
14
15
16
17 In the case of hydrostatic lubrication, the flowrate and pressure in a basic test bench by
18 magnetic field under variable external loads was explored (Hesselbach and Abel-
19 Keilhack, 2003). The same authors studied posteriorly the vibrational response of the
20 bearings as active dampers (Díaz-Tena et al., 2013; Guldbakke and Hesselbach, 2006).
21 Valves (or restrictors) with magnetic fluids for hydrostatic bearings determine the
22 pressure drop in function of flowrate and applied magnetic field ((Songjing et al., 2002)).
23 Results from different MRF and characterization of fluids in valve mode was presented
24 in(Bin Mazlan, 2008)).
25
26
27
28
29
30
31

32 Considering that *ferrofluids* are highly stable but show very low magnetoviscous
33 effect as bearings lubricant ((Urreta et al., 2010)); and that *MRF*, unstable but with very
34 high magnetorheology response, the research presented in this paper was conducted
35 exclusively with MRF. Thus,
36
37
38
39

40 Section 2 describes the modelling and characterization of the magnetic fluid used in
41 the research; Section 3 deals with the mathematical modelling of the active hybrid journal
42 bearing; Section 4 presents the prototypes for experimental validation; Section 5
43 summarizes the results, and finally Section 6 the main conclusions.
44
45
46
47

48 49 CHARACTERIZATION OF 50 MAGNETORHEOLOGICAL FLUIDS 51

52
53
54
55 A commercial magnetorheological fluid from LORD® Corp. model MRF 122-2ED
56 was used in this research. First at all, experimental characterization of the fluid was
57
58
59
60

carried out. Data given by manufacturers are usually approximate values, both for magnetic and rheological behaviour. Therefore the fluid magnetic response was studied, along with the rheological properties under applied magnetic field and temperature.

MRFs are strongly non-Newtonian fluids, presenting a strong yield stress in function of applied magnetic field before fluid flows. The computational model to consider its behaviour was Herschel-Buckley given by Eq. (3), which is the classical Bingham model modified with thinning effect, as shown in Figure 3. Equation (4) is the apparent viscosity of the non-Newtonian fluid, the viscosity that would have a Newtonian fluid with the same shear stress (τ) at that strain rate ($\dot{\gamma}$).

[insert figure 3]

Figure 3 Models for magnetic fluids characterization.

$$\tau = (\tau_0(H) + K|\dot{\gamma}|^{1/m}) \operatorname{sgn}(\dot{\gamma}) \quad (3)$$

$$\mu_{\text{app}} = \tau / \dot{\gamma} \quad (4)$$

The magnetic characterization was performed with a Magnet-Physik Permagraph L magnetometer and the electromagnet EP-3, from which the magnetic field strength, flux density and magnetic fluid permeability were obtained, as shown in Figure 4. The magnetorheological characterization was carried out with a Thermo HAAKE RheoStress RS150 control stress rheometer, with a magnetic module and a thermally controlled plate.

[insert figure 4]

Figure 4 Magnetic characterization of MRF 122–2ED from LORD Corp.

Rheological analysis of the MRF was carried out, and the results are presented in Figure 5, i.e., temperature effect in viscosity and shear thinning effect in function of the

1
2
3 magnetic field; in Figure 6, yield stress and base fluid viscosity in function of applied
4 magnetic field at room temperature.
5
6

7
8 [insert figure 5]
9

10
11
12 Figure 5 Rheological characterization of MRF, temperature and shear thinning effect.
13
14

15
16
17
18 [insert figure 6]
19

20
21
22 Figure 6 Rheological characterization of MRF, shear stress and base viscosity.
23
24

25 26 27 28 29 LUBRICATION MODEL WITH MAGNETIC FLUIDS 30 31

32
33 Mathematical modelling of MRF based lubrication was carried out in this section, in
34 order to improve the designing and optimize the behaviour of the prototypes. Modelling
35 is focused on determining i) pressure in the fluid, ii) velocity distribution (flowrate) and
36 iii) magnetic field in the bearing and valves. The design of the bearing and valve
37 prototypes is discussed in Section 4, together with the test benches for experimental
38 characterization.
39
40
41
42

43
44
45 Calculations and fluid simulations were carried out with two tools, in both cases
46 considering non-Newtonian fluid: a) for two-dimensional models, modified Reynolds
47 equation is solved into a MATLAB® based program, and b) for three-dimensional cases,
48 computational fluid dynamics (CFD) is used with SIEMENS NX® Advanced Flow.
49
50
51
52
53
54
55
56
57
58
59
60
61
62
63
64
65
66
67
68
69
70
71
72
73
74
75
76
77
78
79
80
81
82
83
84
85
86
87
88
89
90
91
92
93
94
95
96
97
98
99
100
101
102
103
104
105
106
107
108
109
110
111
112
113
114
115
116
117
118
119
120
121
122
123
124
125
126
127
128
129
130
131
132
133
134
135
136
137
138
139
140
141
142
143
144
145
146
147
148
149
150
151
152
153
154
155
156
157
158
159
160
161
162
163
164
165
166
167
168
169
170
171
172
173
174
175
176
177
178
179
180
181
182
183
184
185
186
187
188
189
190
191
192
193
194
195
196
197
198
199
200
201
202
203
204
205
206
207
208
209
210
211
212
213
214
215
216
217
218
219
220
221
222
223
224
225
226
227
228
229
230
231
232
233
234
235
236
237
238
239
240
241
242
243
244
245
246
247
248
249
250
251
252
253
254
255
256
257
258
259
260
261
262
263
264
265
266
267
268
269
270
271
272
273
274
275
276
277
278
279
280
281
282
283
284
285
286
287
288
289
290
291
292
293
294
295
296
297
298
299
300
301
302
303
304
305
306
307
308
309
310
311
312
313
314
315
316
317
318
319
320
321
322
323
324
325
326
327
328
329
330
331
332
333
334
335
336
337
338
339
340
341
342
343
344
345
346
347
348
349
350
351
352
353
354
355
356
357
358
359
360
361
362
363
364
365
366
367
368
369
370
371
372
373
374
375
376
377
378
379
380
381
382
383
384
385
386
387
388
389
390
391
392
393
394
395
396
397
398
399
400
401
402
403
404
405
406
407
408
409
410
411
412
413
414
415
416
417
418
419
420
421
422
423
424
425
426
427
428
429
430
431
432
433
434
435
436
437
438
439
440
441
442
443
444
445
446
447
448
449
450
451
452
453
454
455
456
457
458
459
460
461
462
463
464
465
466
467
468
469
470
471
472
473
474
475
476
477
478
479
480
481
482
483
484
485
486
487
488
489
490
491
492
493
494
495
496
497
498
499
500
501
502
503
504
505
506
507
508
509
510
511
512
513
514
515
516
517
518
519
520
521
522
523
524
525
526
527
528
529
530
531
532
533
534
535
536
537
538
539
540
541
542
543
544
545
546
547
548
549
550
551
552
553
554
555
556
557
558
559
560
561
562
563
564
565
566
567
568
569
570
571
572
573
574
575
576
577
578
579
580
581
582
583
584
585
586
587
588
589
590
591
592
593
594
595
596
597
598
599
600
601
602
603
604
605
606
607
608
609
610
611
612
613
614
615
616
617
618
619
620
621
622
623
624
625
626
627
628
629
630
631
632
633
634
635
636
637
638
639
640
641
642
643
644
645
646
647
648
649
650
651
652
653
654
655
656
657
658
659
660
661
662
663
664
665
666
667
668
669
670
671
672
673
674
675
676
677
678
679
680
681
682
683
684
685
686
687
688
689
690
691
692
693
694
695
696
697
698
699
700
701
702
703
704
705
706
707
708
709
710
711
712
713
714
715
716
717
718
719
720
721
722
723
724
725
726
727
728
729
730
731
732
733
734
735
736
737
738
739
740
741
742
743
744
745
746
747
748
749
750
751
752
753
754
755
756
757
758
759
760
761
762
763
764
765
766
767
768
769
770
771
772
773
774
775
776
777
778
779
780
781
782
783
784
785
786
787
788
789
790
791
792
793
794
795
796
797
798
799
800
801
802
803
804
805
806
807
808
809
810
811
812
813
814
815
816
817
818
819
820
821
822
823
824
825
826
827
828
829
830
831
832
833
834
835
836
837
838
839
840
841
842
843
844
845
846
847
848
849
850
851
852
853
854
855
856
857
858
859
860
861
862
863
864
865
866
867
868
869
870
871
872
873
874
875
876
877
878
879
880
881
882
883
884
885
886
887
888
889
890
891
892
893
894
895
896
897
898
899
900
901
902
903
904
905
906
907
908
909
910
911
912
913
914
915
916
917
918
919
920
921
922
923
924
925
926
927
928
929
930
931
932
933
934
935
936
937
938
939
940
941
942
943
944
945
946
947
948
949
950
951
952
953
954
955
956
957
958
959
960
961
962
963
964
965
966
967
968
969
970
971
972
973
974
975
976
977
978
979
980
981
982
983
984
985
986
987
988
989
990
991
992
993
994
995
996
997
998
999
1000

Modelling was applied to two elements, described in the following two sub-sections:
 1) Hybrid journal bearings and 2) magnetorheological (MR) valves.

Hybrid journal bearing lubricated with MRF

The solution of lubrication with magnetic fluids is based in a modified Reynolds equation, where the behaviour of the fluid ranges from Newtonian to non-Newtonian response. To solve the modified Reynolds equation, principles studied by (Dorier and Tichy, 1992; Tichy, 1991) were assumed, modifying the Bingham equation for the Herschel-Buckley model.

In the MRF lubrication, strong fluid yield stress requires a non-linear approach for solving the model. In this case, the shear stress in the fluid is evaluated across the gap radial section to determine the zone where the fluid is flowing and where it is plug. In Figure 7 the zones I and II are flowing; and in the zone III there is plug fluid (or pseudo-plastic MRF):

[insert figure 7]

Figure 7 Balance of forces on a fluid element in the plug region, MRF lubrication

Considering equations (1), (3), and (4), the Reynolds equation, Herschel-Buckley model and apparent viscosity respectively, the equation to solve is:

$$\frac{\partial p}{\partial \theta} = 6 \mu_{app} \rho R^2 \omega \frac{h-h^*}{h^3} \quad (5)$$

Considering the behaviour of MRF fluids, and the plug formation under magnetic field, velocity distribution of the fluid is defined with next equations, see Figure 8:

$$I) \quad u_x(y) = \frac{1}{2} \left(-\frac{1}{K} \frac{dp}{dx} \right) \left[h_a^2 - (h_a - y)^2 \right] \quad (0 \leq y \leq h_a) \quad (6)$$

$$II) \quad u_x(y) = \frac{1}{2} \left(-\frac{1}{K} \frac{dp}{dx} \right) \left[(h - h_b)^2 - (y - h_b)^2 \right] \quad (h_b \leq y \leq h) \quad (7)$$

$$\text{III) } u_x(y) = \frac{1}{2} \left(-\frac{1}{K} \frac{dp}{dx} \right) h_a^2 \quad (h_a \leq y \leq h_b) \quad (8)$$

[insert figure 8]

Figure 8 Velocity distribution in a MRF under magnetic field with plug region (III)

Where the overall flow-rate in the bearing is:

$$Q = \left(\int_0^{h_a} u_x(0 < y < h_a) dy + \int_{h_b}^h u_x(h_b < y < h) dy + \int_{h_a}^{h_b} u_x(h_a < y < h_b) dy \right) L \quad (9)$$

The modified Reynolds equation is solved numerically by finite difference method, in which the bearing is discretized in “n” elements (i, j), and the equilibrium equation is solved (10).

$$A_0 P_{i,j} = A_1 P_{i+1,j} + A_2 P_{i-1,j} + A_3 P_{i,j+1} + A_4 P_{i,j-1} + B \quad (10)$$

Solving this equation, the pressure profile (Figure 9), the velocity distribution of the magnetic fluid in the bearing and therefore the load capacity, stiffness and flowrate were obtained.

[insert figure 9]

Figure 9 Pressure distribution (a) and gradient (b) into a journal bearing, solution in 3D graph.

Reynolds-based modelling was used for two-dimensional cases, like plain journal bearings. In the case of three dimensional models like hybrid bearings with recesses and the MR valve, the CFD tool was implemented with Herschel-Buckley model for non-Newtonian fluids, which is modified to be solved at any shear stress with a base viscosity (11). It means that below a certain shear rate value, viscosity is Newtonian and given by user (μ_0), and above that value, the viscosity is calculated for each element.

$$\mu = \mu_0 \quad 0 \leq \dot{\gamma} \leq \frac{\tau_i}{\mu_0}$$

$$\mu = K + \frac{\tau_0}{\dot{\gamma}} \quad \dot{\gamma} > \frac{\tau_i}{\mu_0}$$
(11)

Active magnetorheological (MR) valves

Magnetorheological (MR) valve was calculated with CFD software, where the pressure drop in the valve was determined for different flowrates and applied magnetic fields. As shown in Figure 10, the valve has a coaxial architecture with two squeeze surfaces where pressure drop and flowrate was controlled. Moreover, velocity and flowrate of the fluid were calculated as shown in Figure 10b.

Magnetic calculations were carried out to determine the magnetization of the fluid. Figure 11 shows the magnetic simulation of the MR valve, which was designed for the hybrid journal bearing, with the magnetic flux density plotted for some critical points of the valve.

[insert figure 10]

Figure 10 CFD simulations of MR valve, pressure drop (a) and flow-rate calculation (b).

[insert figure 11]

Figure 11 Magnetic simulation of MR valve (a) and magnetic field in control points (b).

DESING OF PROTOTYPE AND TEST BENCH

Being the main aim of this research the development of magnetic fluid based technology for machine-tool active spindles, two kind of devices were tested: a) magnetorheological valves for active lubrication, and b) a hybrid journal bearing with active compensation.

Magnetorheological (MR) valves

Four MR valves were dimensioned and designed to be used in the hybrid journal bearing that will be described in the next section. Each of the four valves was composed of two commercial electromagnets with coaxial architecture, in which the fluid flows through two squeeze areas where the magnetic field is concentrated. Figure 12 shows the valve and main design parameters

[insert figure 12]

Figure 12 MR valve for hybrid bearing, design sketches (a) and working principle (b).

The gap for the fluid is 0.6mm, the external diameter (D_{ext}) is 30mm and the internal diameter of squeeze area under magnetic field (D_{int}) is 24mm. Coils used in the valve had 850 turns of 0.15mm diameter wires, for a maximum 5A current, so that, as shown in Figure 11(a) the field induced in the fluid it is up to 800mT. In Figure 13 the valves and parts are shown.

[insert figure 13]

Figure 13 MR valves picture with description of parts

Hybrid journal bearing

The hybrid journal bearing demonstrator was composed by two main parts: the main structure with electric motor, main shaft and bed (the test bench), and the prototype of bearing system with monitoring and magnetic systems, see Figure 14.

[insert figure 14]

Figure 14 Sketch of hybrid journal bearing test bench and prototype

The main shaft was guided by high precision rolling bearings with runout below $2\mu\text{m}$, and a semi-shaft was attached to be tested into the bearing, as shown in Figure 15. The shaft was driven by an electric motor, with two transmission belts. The system was clamped onto a heavy and stiff table to ensure stability. The bearing was made in bronze to ensure good tribological properties and to guide properly the magnetic field generated by two coils into the MRF. This system was mounted in the bearing house, which was guided with two perpendicular linear rolling guides to ensure two degrees of freedom between bearing and shaft, radial movement.

Load was applied radially on the bearing with a screw and a load cell (INTERFACE SM 20kN), and the displacements derived by the load were measured with two eddy current probes (Brüel&Kjaer SD-081) with a resolution below $1\mu\text{m}$.

[insert figure 15]

Figure 15 Hybrid journal bearing test bench, overall view

[insert figure 16]

Figure 16 Hybrid journal bearing prototype, bearing house section view and dimensions

1
2
3 Figure 16 shows a detailed view of the bearing house and active bearing system, and
4 the main geometrical values of the hybrid bearing and recesses.
5
6

7
8 The four magnetorheological valves shown in previous section were located close to
9 the bearing house. Valves were working in closed-loop control with a real-time
10 controller, INGETEAM IC3. The control diagram is shown in Figure 17. Each valve had
11 its signal amplifiers providing up to 5A with 24V, while the fluid was pumped with a
12 hydraulic system composed by a pump/tank module and a pressure relief valve.
13
14
15
16

17
18 [insert figure 17]
19

20
21 Figure 17 Active hybrid journal bearings hydraulic circuit and control
22
23

24 25 26 27 RESULTS AND DISCUSSION 28

29
30 The results are split into two sections: magnetorheological (MR) valves and active
31 hybrid journal bearing.
32
33

34 35 36 Magnetorheological valves 37

38
39 Calculations were carried out with CFD due to the complexity of the flow into the
40 channels, and they were compared with experimental results from the prototype. The first
41 step was the calculation of magnetic field into the valve (see Figure 11), with flux density
42 isovalues (a) and some control points in function of the current through the coils. After
43 calculating the magnetic field values, the expected rheology of MRF was determined
44 based on the experimental results (see Figure 5 and Figure 6). The final step was the
45 computation in CFD of the flow rate and pressure drop in to the MR valve. To achieve
46 right results from simulations, the viscosity for low shear rate (μ_0) was adjusted, a value
47 selected in the computation to solve Navier-Stokes equations including Herschel-Buckley
48
49
50
51
52
53
54
55
56
57
58
59
60

1
2
3 model, equation (11). A good agreement was achieved with a constant ratio in all the
4
5 simulations of $\frac{\tau_0}{Q \cdot \mu_0} \approx 200$ (see Figure 18).
6
7

8
9 [insert figure 18]
10

11
12
13 Figure 18 Experimental and theoretical results in the MR valve for active bearing
14

15 16 17 Active hybrid bearing

18
19
20 The experimental analysis of the active hybrid journal bearing was carried out
21
22 regarding three aspects: load capacity, time response and wear during operation.
23

24 25 Load capacity and stiffness of the active hybrid journal bearing

26
27
28 Load capacity and stiffness in the active hybrid bearings were experimentally studied
29
30 in two ways: 1) the hydrodynamic effect improvement due to the magnetic fluid flow in
31
32 the bearing, and 2) the hydrostatic response with the four MR valves feeding the recesses
33
34 and working in closed loop control.
35

36
37 To determinate the hydrodynamic active response, the first step was to calculate the
38
39 magnetic field intensity in the clearance, where the results for a half model of the system
40
41 (symmetry assumption) are shown in Figure 19:
42

43 [insert figure 19]
44

45
46 Figure 19 Magnetic field in the hybrid bearing (a), and field strength in the gap (b)
47
48 for cutting plane defined by (b), half cylinder.
49

50
51
52 With those magnetic field values and the magnetic fluid model implemented in the
53
54 modified Reynolds equation (5), hydrodynamic response was evaluated for MRF, and
55
56 compared with experimental results, see Figure 20 and Figure 21. The tests were carried
57
58 out at two rotational speeds: 50 rpm and 200rpm.
59
60

[insert figure 20]

Figure 20 Hybrid bearing, shaft eccentricity path for 50rpm (a) and 200rpm (b).

[insert figure 21]

Figure 21 Hybrid journal bearing, load capacity for 50rpm (a) and 200rpm (b).

As shown in Figure 20 and Figure 21, magnetic fluid lubrication improves the hydrodynamic behaviour, increasing the load capacity and stiffness by at least 50% for eccentricity values around $0.4 < \epsilon < 0.7$, and the shaft displacement was much more linear than in classical hydrodynamic bearings, with much lower cross movement.

Second experimental tests were performed to determine the system behaviour working with active hydrostatic lubrication (four MR valves), using MRF as lubricant (Figure 17). The load was applied in two directions, aligned with the recesses and at 45° , as shown in Figure 22(a), and with or without rotational speed in Figure 22 (b), hydrostatic or hydrodynamic. The lubricant pressure achieved in the hybrid bearing for the two directions is shown in Figure 23(a) and (b).

[insert figure 22]

Figure 22 Hybrid bearing, direction of the applied load (a), pressure graph with or without rotational velocity (b)

[insert figure 23]

Figure 23 Pressure distribution in the hybrid bearing for aligned (a) and 45° oriented

1
2
3 load (b)
4
5
6
7
8
9

10 As presented in Figure 24, below a critical load (in function of the force direction) the
11 stiffness of the active bearing for static loads is quasi-infinite, with typical signal noise
12 coming from movement of the shaft (unbalance) and monitoring (signal noise), in this
13 case $\pm 5\%$ of clearance. Once critical load is overcome, the stiffness is reduced
14 dramatically in the case of pure hydrostatic lubrication, and in hybrid condition (200r/min
15 in the tests) the load can be still increased due to hydrodynamic pressure Figure 24.
16 Maximum loads were between 600N and 1200N in function of mentioned rotational
17 velocity and applied force direction. The loads were only presented till eccentricity of
18 0.75, above that load/displacement the results were not reliable.
19
20
21
22
23
24
25

26
27 [insert figure 24]
28
29

30 Figure 24 Experimental results of active hybrid bearing under load, stationary values.
31
32

33 Time response of active hybrid journal bearing 34

35
36 The system time response was further tested to determine the capability of this active
37 hybrid journal bearing for compensation of dynamic loads. The tests were carried out
38 applying a command to the valves and measuring the movement in the shaft, obtaining
39 the response between current in the coils and the displacement in the shaft.
40
41
42
43
44

45 [insert figure 25]
46
47

48 Figure 25 Experimental results of time response in active hybrid bearing.
49
50

51 As shown in Figure 25, the time constant of both axes was in the range of 0.06-0.07s,
52 slight differences from hydraulic and experimental set-up. Therefore, the resulting system
53 bandwidth (3dB point) was below 3Hz. With those values, active control by magnetic
54 fluids cannot be considered for compensation of higher frequency perturbations. For
55
56
57
58
59
60

1
2
3 example, in grinding or turning spindles the rotational speed is around 2000r/min, and the
4 compensation of the shaft unbalance would require frequency around 33Hz, more than
5 ten times higher than available in this system. But the capability to achieve quasi-infinite
6 stiffness under static loads, and therefore maximum precision in guiding system, was
7 demonstrated.
8
9

10 11 12 13 Bearing and shaft wear during operation 14 15

16
17 Finally, the bearing and shaft surface wear were analysed. Magnetic fluids are not
18 optimal lubricants, since magnetic particles in suspension do not have good friction and
19 wear properties. The effect in the surface roughness during 1000hr operation in the test
20 bench was measured in four testing zones, as presented in Figure 26 (a) for bearing and
21 (b) for the shaft:
22
23
24

25
26 [insert figure 26]
27
28

29 Figure 26 Wear and roughness measuring zones, a) bearing and b) shaft.
30
31

32
33 Roughness values (R_a and R_z) of the bearing and the shaft were measured in the long
34 time test of 1000hr, with periodical measurements, leading to the values presented in
35 Figure 27:
36
37

38
39 [insert figure 27]
40
41

42 Figure 27 Roughness values in the shaft, a) averaged roughness (R_a), and b) maximum
43 roughness (R_z)
44
45

46
47
48
49 [insert figure 28]
50
51

52 Figure 28 Roughness values in the bearing, a) averaged roughness (R_a), and b)
53 maximum roughness (R_z).
54
55
56
57
58
59
60

1
2
3 As shown in Figure 27 (a) and (b), the shaft roughness was not altered during the test.
4
5 The bearing showed a high roughness in the zone/line labelled as 2, see **Error!**
6
7 **Reference source not found.** (a) and (b), which was due to a scratch manipulating the
8 bearing before the test. The roughness in the other three lines had a slight increase, which
9 could be due to wear caused by magnetic particles in suspension.
10
11

12 CONCLUSIONS

13
14
15
16
17 The use of magnetorheological fluids as active elements in hybrid journal bearings
18 was analysed in this research work. Some prototypes have been developed, and the
19 validity of simulation models and the final performance of the systems were
20 demonstrated experimentally.
21
22
23

- 24
25 • A magnetorheological fluid was experimentally analysed, obtaining deeper
26 information about its behaviour than offered by the manufacturers; as a matter
27 of fact, for studies in the field of magnetic fluids, such a detailed experimental
28 characterization is highly recommended.
29
30
- 31 • Magneto-rheological valves were developed for a full prototype solution in
32 active bearing lubrication. Good agreement between theoretical values and
33 experimental results in terms of pressure drop and flowrate was achieved.
34
35
- 36 • An active hybrid journal bearing was developed, with active hydrodynamic
37 effect and the use of magnetorheological valves. Hydrodynamic effect was
38 improved around 50%, while the active hydrostatic lubrication achieved quasi-
39 infinite static stiffness within a load range.
40
41
- 42 • Transient response of the active bearing is too slow for dynamic loads with a
43 bandwidth lower than 5Hz. It cannot be thus used for active compensation of
44 the unbalance in machine tool spindles shafts.
45
46
47
48
49
50
51
52
53
54
55
56
57
58
59
60

- Bearing and shaft wear rate was analysed, where a slightly roughness increment was monitored after 1000hr test in the bearing, and nothing relevant in the shaft.

REFERENCES

- Aguirre, G., Al-Bender, F., Van Brussel, H., 2010. A multiphysics model for optimizing the design of active aerostatic thrust bearings. *Precision Engineering* 34, 507–515.
- Albers, A., Nguyen, H.T., Burger, W., 2011. Energy efficient hydrodynamic journal bearing by means of closed loop controlled lubrication flow. *Proceedings of ASME/STLE 2011*. Presented at the IJTC2011 International Joint Tribology Conference, Los Angeles, California USA.
- Bassani, R., Piccigallo, B., 1992. *Hydrostatic Lubrication*, Tribology Series. Elsevier, Pisa University, Italy.
- Bin Mazlan, S.A., 2008. The behaviour of magnetorheological fluids in squeeze mode (Thesis for PhD degree). Dublin City University. School of Mechanical and Manufacturing Engineering.
- Bouزيدane, A., Lakis, A.A., Thomas, M., 2008. Nonlinear Dynamic Behavior of a Rigid Rotor Supported by Hydrostatic Squeeze Film Dampers. *J. Tribol.* 130, 041102–041102. doi:10.1115/1.2958079
- Deckler, D.C, Veillette R.J., 2004. Simulation and Control of an Active Tilting-Pad Journal Bearing. *Tribology Transactions - TRIBOL TRANS* 47, 440–458. doi:10.1080/05698190490463277
- Díaz-Tena, E., Marcaide, L.N.L. de L., Gómez, F.J.C., Bocanegra, D.L.C., 2013. Use of Magnetorheological Fluids for Vibration Reduction on the Milling of Thin Floor Parts. *Procedia Engineering, The Manufacturing Engineering Society International Conference, MESIC 2013* 63, 835–842. doi:10.1016/j.proeng.2013.08.252
- Dorier, C., Tichy, J., 1992. Behavior of a bingham-like viscous fluid in lubrication flows. *Journal of Non-Newtonian Fluid Mechanics* 45, 291–310. doi:10.1016/0377-0257(92)80065-6

- 1
2
3 Estupiñan, E.A., Santos, I.F., 2009. Linking rigid multibody systems via controllable thin
4 fluid films. *Tribology International* 42, 1478–1486.
5 doi:10.1016/j.triboint.2009.05.009
6
7
8 Frêne, J., Nicolas, D., Degueurce, B., Berthe, D., Godet, M., 1997. *Hydrodynamic
9 Lubrication: Bearings and Thrust bearings*, Tribology Series. Elsevier, Poitiers,
10 France.
11
12 G. Nikolakopoulos, P., Papadopoulos, C.A., 1998. Controllable high speed journal
13 bearings, lubricated with electro-rheological fluids. An analytical and
14 experimental approach. *Tribology International* 31, 225–234. doi:10.1016/S0301-
15 679X(98)00025-5
16
17
18 Guldbakke, J.M., Hesselbach, J., 2006. Development of bearings and a damper based on
19 magnetically controllable fluids. *J. Phys.: Condens. Matter* 18, S2959.
20 doi:10.1088/0953-8984/18/38/S29
21
22
23 Hesselbach, J., Abel-Keilhack, C., 2003. Active hydrostatic bearing with
24 magnetorheological fluid. *Journal of Applied Physics* 93, 8441–8443.
25 doi:10.1063/1.1555850
26
27
28 Hsu, T.-C., Chen, J.-H., Chiang, H.-L., Chou, T.-L., 2013. Lubrication performance of
29 short journal bearings considering the effects of surface roughness and magnetic
30 field. *Tribology International* 61, 169–175. doi:10.1016/j.triboint.2012.12.016
31
32
33 Jordan, M.A., 2000. Experimental results and implications of perturbation testing with
34 servofluid control bearings. *Orbit* 2nd Quarter, 10–17.
35
36
37 Kuzhir, P.P., Kuzhir, P.G., Gul'kov, G.I., Rudenya, A.L., 2011. Determination of the free
38 boundary of the lubricant layer of a ferrofluid bearing. *J Eng Phys Thermophy* 84,
39 422–429. doi:10.1007/s10891-011-0488-6
40
41
42 Morosi, S., Santos, I.F., 2011. Active lubrication applied to radial gas journal bearings.
43 Part 1: Modeling. *Tribology International* 44, 1949–1958.
44 doi:10.1016/j.triboint.2011.08.007
45
46
47 Nicoletti, R., Santos, I.F., 2008. Control System Design for Flexible Rotors Supported by
48 Actively Lubricated Bearings. *Journal of Vibration and Control* 14, 347–374.
49 doi:10.1177/1077546307080014
50
51
52 Nicoletti, R., Santos, I.F., 2003. Linear and non-linear control techniques applied to
53 actively lubricated journal bearings. *Journal of Sound and Vibration* 260, 927–
54 947. doi:10.1016/S0022-460X(02)00951-3
55
56
57 Odenbach, S., 2002. *Magnetoviscous Effects in Ferrofluids*, Lecture Notes in Physics.
58 Springer.
59
60

- 1
2
3 Osman, T.A., 2001. Misalignment Effect on the Static Characteristics of Magnetized
4 Journal Bearing Lubricated with Ferrofluid. *Tribology Letters* 11, 195–203.
5 doi:10.1023/A:1012548624183
6
7
8 Osman, T.A., Nada, G.S., Safar, Z.S., 2001. Effect of Using Current-Carrying-Wire
9 Models in the Design of Hydrodynamic Journal Bearings Lubricated with
10 Ferrofluid. *Tribology Letters* 11, 61–70. doi:10.1023/A:1016657914947
11
12
13 Osman, T.A., Nada, G.S., Safar, Z.S., 2001. Static and dynamic characteristics of
14 magnetized journal bearings lubricated with ferrofluid. *Tribology International*
15 34, 369–380. doi:10.1016/S0301-679X(01)00017-2
16
17
18 Peng, J., Zhu, K.-Q., 2005. Hydrodynamic Characteristics of ER Journal Bearings with
19 External Electric Field Imposed on the Contractive Part. *Journal of Intelligent*
20 *Material Systems and Structures* 16, 493–499. doi:10.1177/1045389X05052312
21
22
23 Reynolds, O., 1886. On the Theory of Lubrication and Its Application to Mr. Beauchamp
24 Tower's Experiments, Including an Experimental Determination of the Viscosity
25 of Olive Oil. *Phil. Trans. R. Soc. Lond.* 177, 157–234. doi:10.1098/rstl.1886.0005
26
27
28 Santos, I.F., Watanabe, F.Y., 2006. Lateral dynamics and stability analysis of a gas
29 compressor supported by hybrid and active lubricated multirecess journal bearing.
30 *Journal of the Brazilian Society of Mechanical Sciences and Engineering* 28, 485–
31 495. doi:10.1590/S1678-58782006000400014
32
33
34 Shamoto, E., Suzuki, N., Hamaguchi, A., 2006. A New Fluid Bearing Utilizing Traveling
35 Waves. *CIRP Annals - Manufacturing Technology* 55, 411–414.
36 doi:10.1016/S0007-8506(07)60447-8
37
38
39 Songjing, L., Guanghuai, W., Dong, C., Songying, L., 2002. New type relief valve using
40 magneto-rheological fluid.
41
42
43 Spur, G., Patzwald, R., 1998. Lubrication of hydrodynamic journal bearings with
44 magnetic fluids. *Production Engineering - Annals of the German Academic*
45 *Society for Production Engineering (WGP) V/1*, 47–51.
46
47
48 Sun, L., Krodkiewski, J.M., 1999. Experimental verification of modelling and analysis of
49 the dynamic properties of an active journal bearing. 10th World congress on the
50 theory of machines and mechanisms, Olulu, Finland.
51
52
53 Tichy, J.A., 1991. Hydrodynamic lubrication theory for the Bingham plastic flow model.
54 *Journal of Rheology* 35, 477–496. doi:10.1122/1.550231
55
56
57 Uhlmann, E., Bayat, N., 2003. Applications of ferrofluids in bearings and positioning
58 system. *Production Engineering - Annals of the German Academic Society for*
59 *Production Engineering (WGP) 10*, 125–128.
60

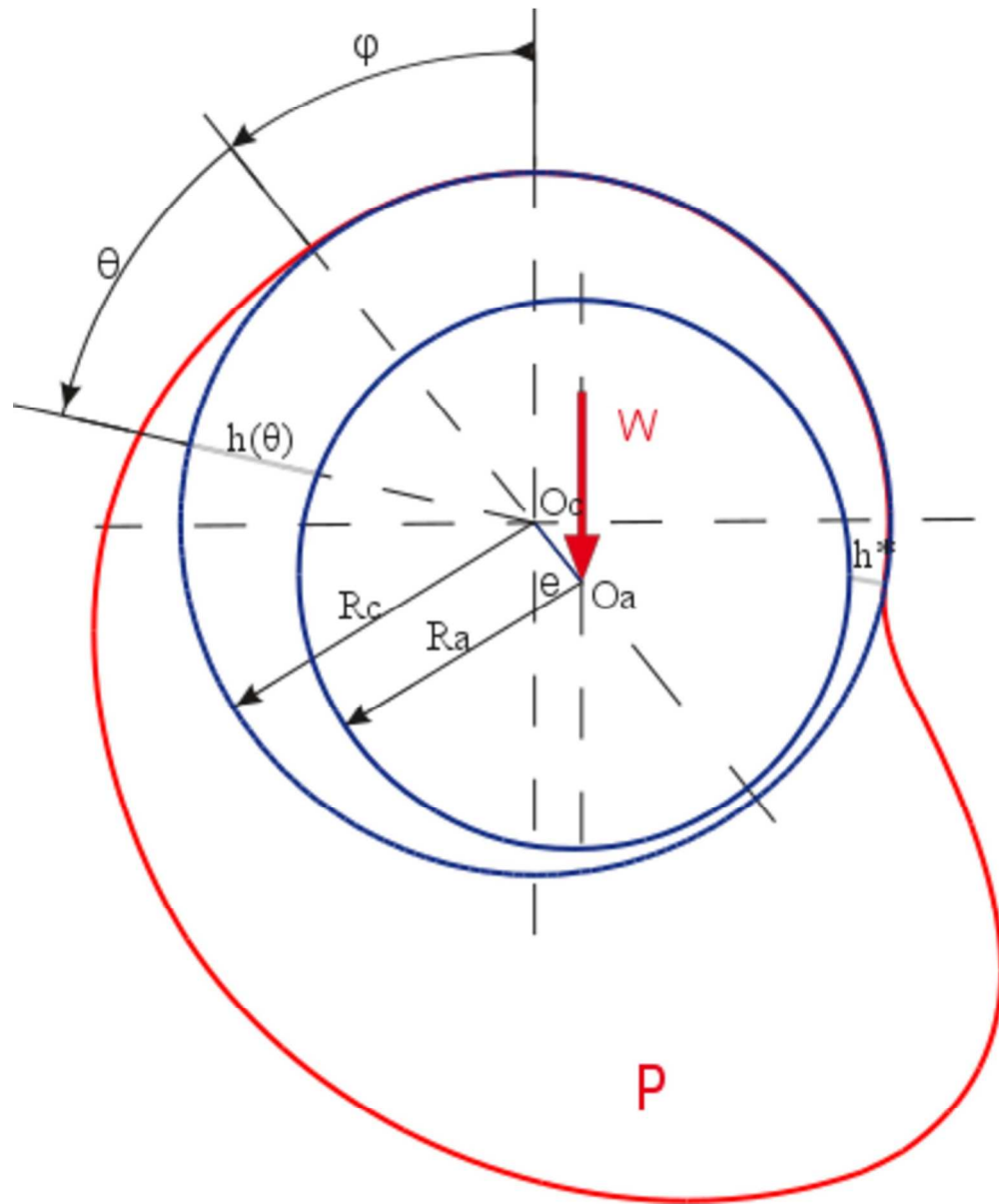
1
2
3 Uhlmann, E., Spur, G., Bayat, N., Patzwald, R., 2002. Application of magnetic fluids in
4 tribotechnical systems. *Journal of Magnetism and Magnetic Materials* 252, 336–
5 340. doi:10.1016/S0304-8853(02)00724-2
6
7

8 Urreta, H., Leicht, Z., Sanchez, A., Agirre, A., Kuzhir, P., Magnac, G., 2010.
9 Hydrodynamic Bearing Lubricated with Magnetic Fluids. *Journal of Intelligent*
10 *Material Systems and Structures* 21, 1491–1499.
11 doi:10.1177/1045389X09356007
12

13
14 Weck, M., 1984. *Handbook of Machine Tools*. John Wiley & Sons Ltd, Chichester West
15 Sussex ; New York.
16
17

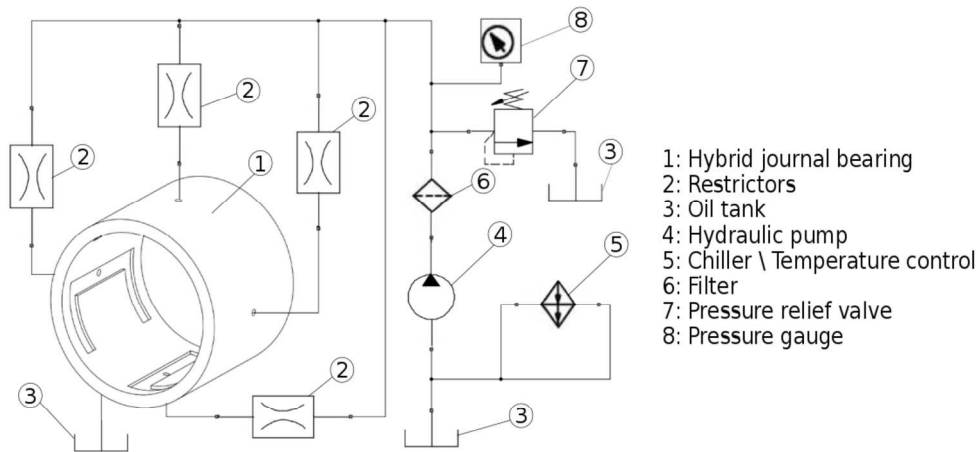
18
19
20
21
22
23
24
25
26
27
28
29
30
31
32
33
34
35
36
37
38
39
40
41
42
43
44
45
46
47
48
49
50
51
52
53
54
55
56
57
58
59
60

For Peer Review



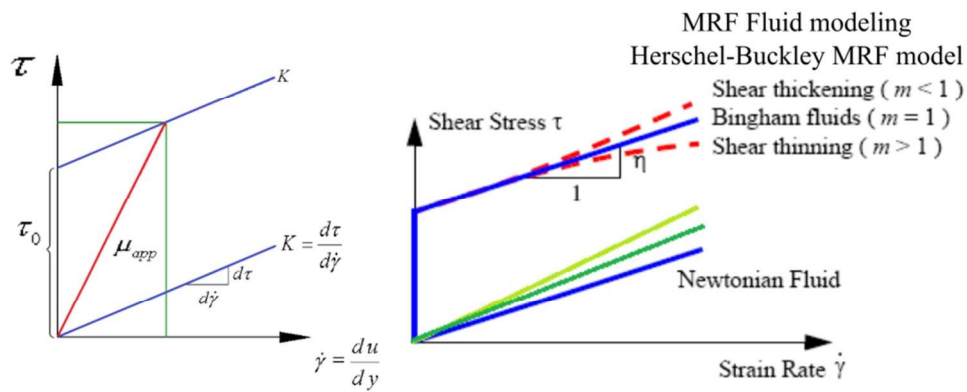
Hydrodynamic pressure in journal bearing
[insert figure 1]
130x157mm (300 x 300 DPI)

1
2
3
4
5
6
7
8
9
10
11
12
13
14
15
16
17
18
19
20
21
22
23
24
25
26
27
28
29
30
31
32
33
34
35
36
37
38
39
40
41
42
43
44
45
46
47
48
49
50
51
52
53
54
55
56
57
58
59
60



Hhybrid journal bearing and hydraulic circuit
 [insert figure 2]
 233x168mm (300 x 300 DPI)

Review

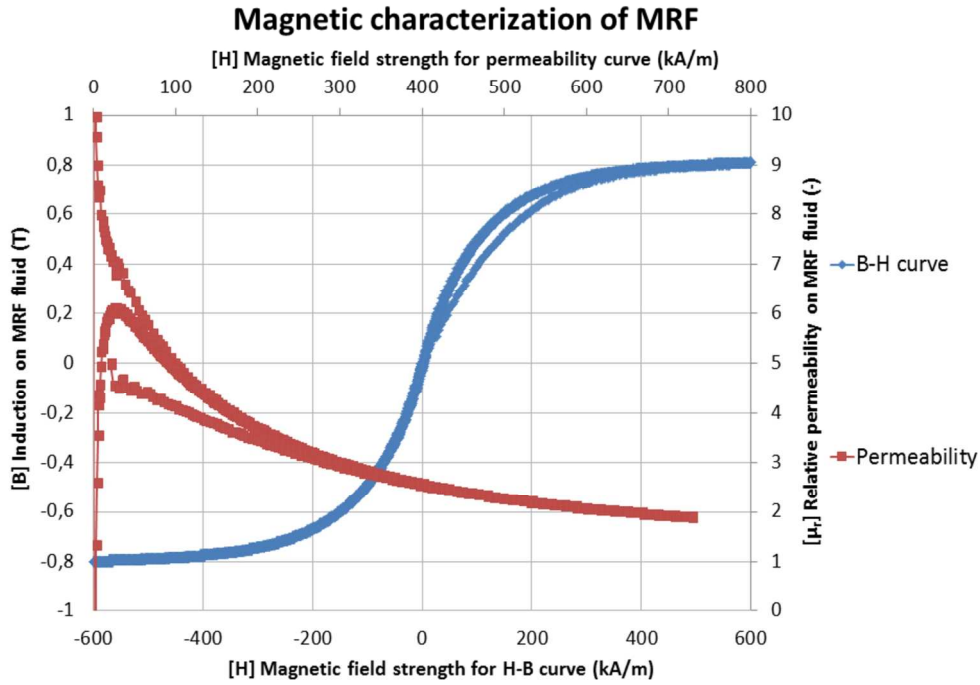


Models for magnetic fluids characterization
 [insert figure 3]
 111x45mm (300 x 300 DPI)

Peer Review

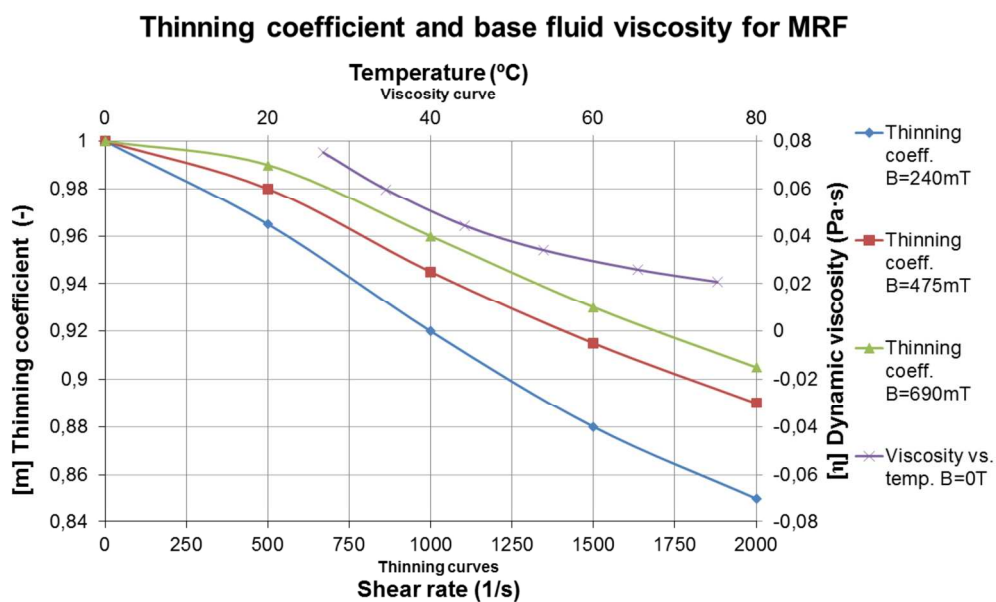
1
2
3
4
5
6
7
8
9
10
11
12
13
14
15
16
17
18
19
20
21
22
23
24
25
26
27
28
29
30
31
32
33
34
35
36
37
38
39
40
41
42
43
44
45
46
47
48
49
50
51
52
53
54
55
56
57
58
59
60

1
2
3
4
5
6
7
8
9
10
11
12
13
14
15
16
17
18
19
20
21
22
23
24
25
26
27
28
29
30
31
32
33
34
35
36
37
38
39
40
41
42
43
44
45
46
47
48
49
50
51
52
53
54
55
56
57
58
59
60



Magnetic characterization of MRF 122-2ED from LORD Corp
[insert figure 4]
192x136mm (300 x 300 DPI)

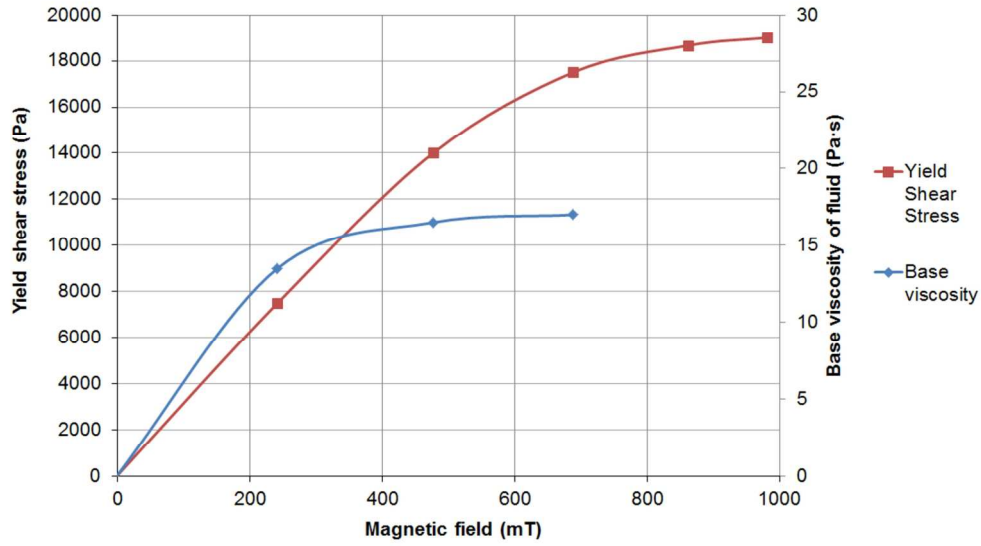
Review



Rheological characterization of MRF, temperature and shear thinning effect
 [insert figure 5]
 201x124mm (300 x 300 DPI)

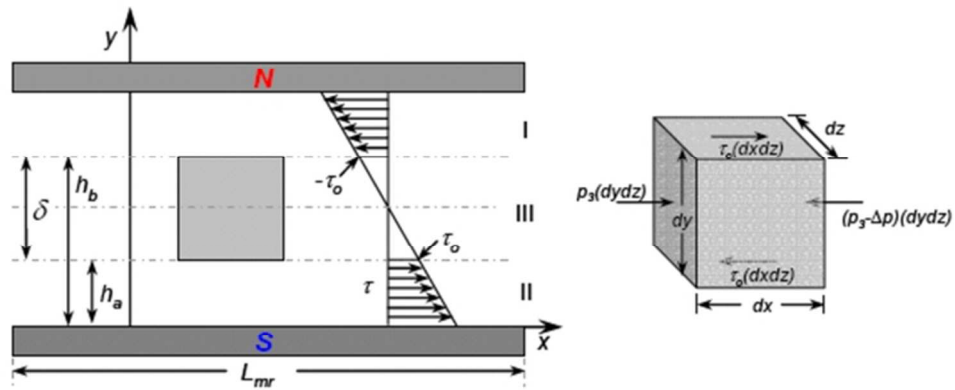
1
2
3
4
5
6
7
8
9
10
11
12
13
14
15
16
17
18
19
20
21
22
23
24
25
26
27
28
29
30
31
32
33
34
35
36
37
38
39
40
41
42
43
44
45
46
47
48
49
50
51
52
53
54
55
56
57
58
59
60

MRF122 fluid's magnetorheological characterization



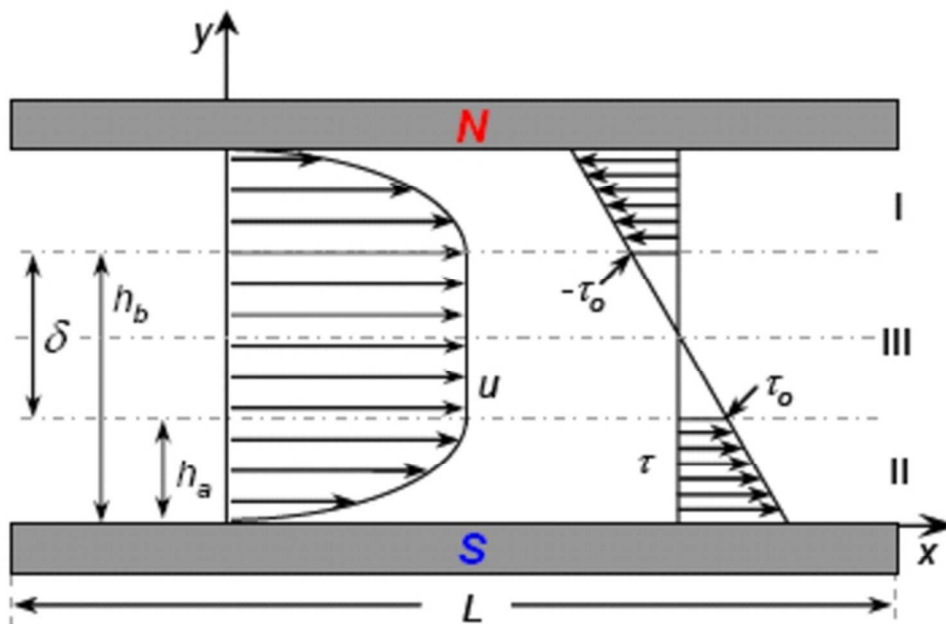
Rheological characterization of MRF, shear stress and base viscosity
[insert figure 6]
179x110mm (300 x 300 DPI)

Review



Balance of forces on a fluid element in the plug region, MRF lubrication
 [insert figure 7]
 63x28mm (300 x 300 DPI)

1
2
3
4
5
6
7
8
9
10
11
12
13
14
15
16
17
18
19
20
21
22
23
24
25
26
27
28
29
30
31
32
33
34
35
36
37
38
39
40
41
42
43
44
45
46
47
48
49
50
51
52
53
54
55
56
57
58
59
60

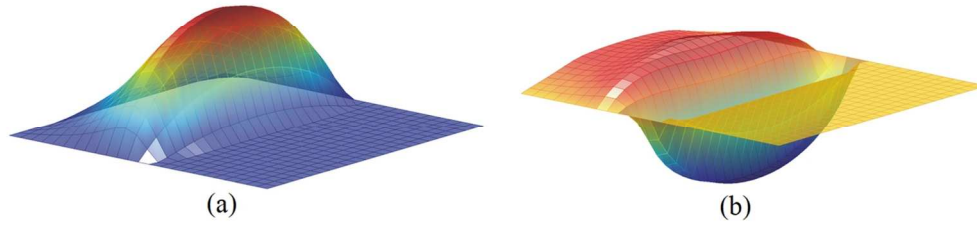


Velocity distribution in a MRF under magnetic field with plug region (III)

[insert figure 8]

57x37mm (300 x 300 DPI)

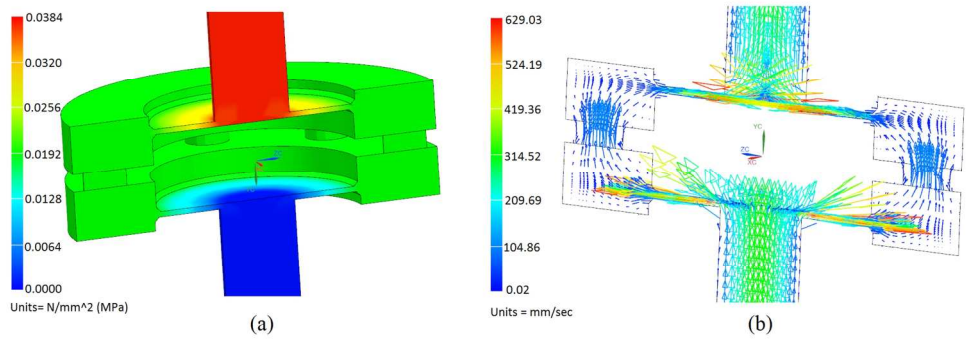
Review



Pressure distribution (a) and gradient (b) into a journal bearing, solution in 3D graph
[insert figure 9]
131x39mm (300 x 300 DPI)

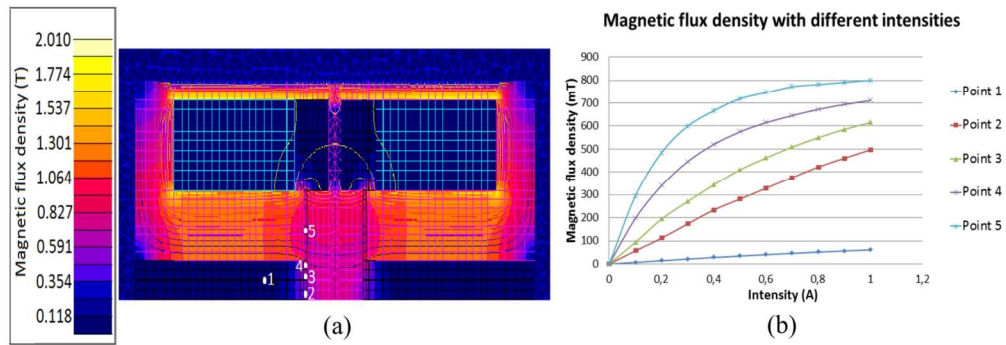
or Peer Review

1
2
3
4
5
6
7
8
9
10
11
12
13
14
15
16
17
18
19
20
21
22
23
24
25
26
27
28
29
30
31
32
33
34
35
36
37
38
39
40
41
42
43
44
45
46
47
48
49
50
51
52
53
54
55
56
57
58
59
60



CFD simulations of MR valve, pressure drop (a) and flow-rate calculation (b)
[insert figure 10]
205x76mm (300 x 300 DPI)

Peer Review

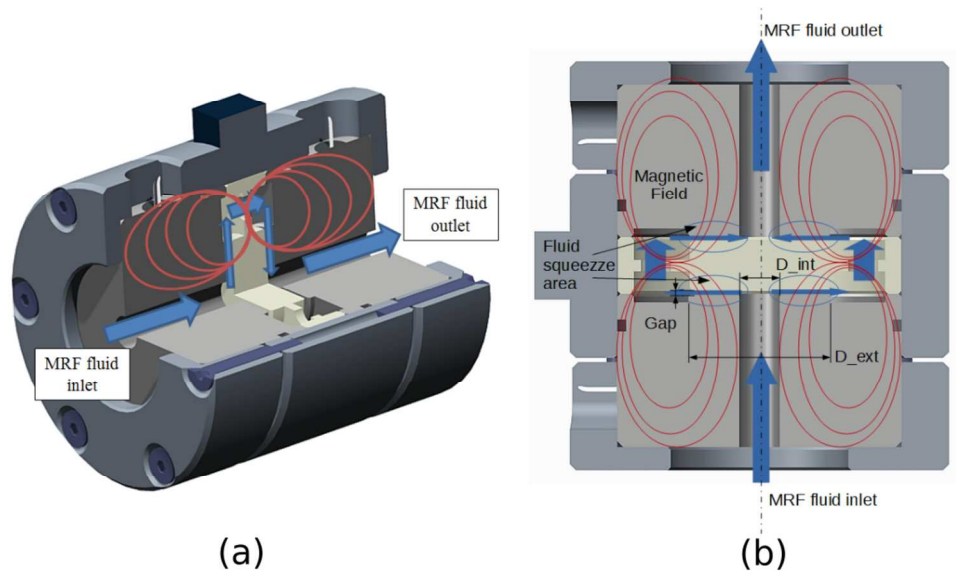


Magnetic simulation of MR valve (a) and magnetic field in control points (b)

[insert figure 11]

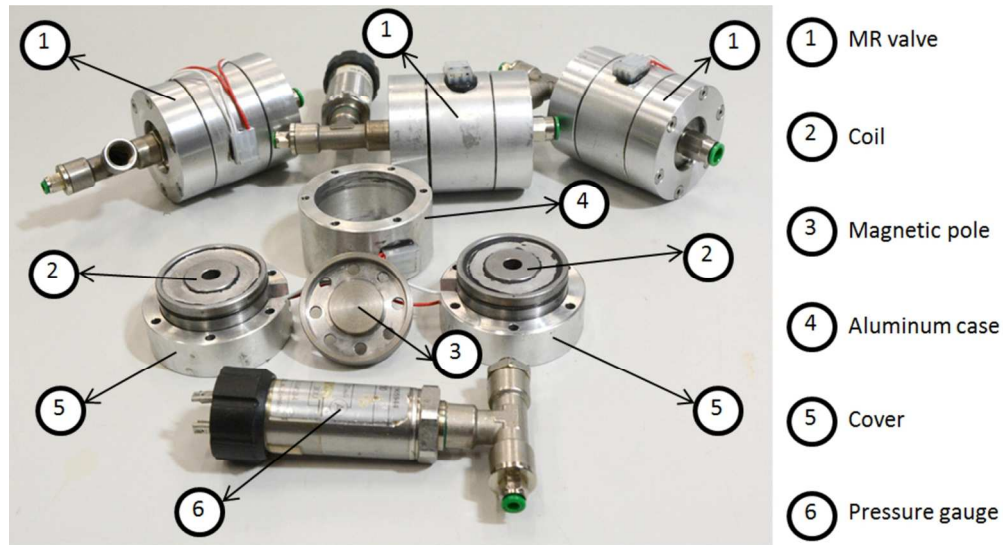
173x61mm (300 x 300 DPI)

1
2
3
4
5
6
7
8
9
10
11
12
13
14
15
16
17
18
19
20
21
22
23
24
25
26
27
28
29
30
31
32
33
34
35
36
37
38
39
40
41
42
43
44
45
46
47
48
49
50
51
52
53
54
55
56
57
58
59
60



MR valve for hybrid bearing, design sketches (a) and working principle (b)
[insert figure 12]
190x107mm (300 x 300 DPI)

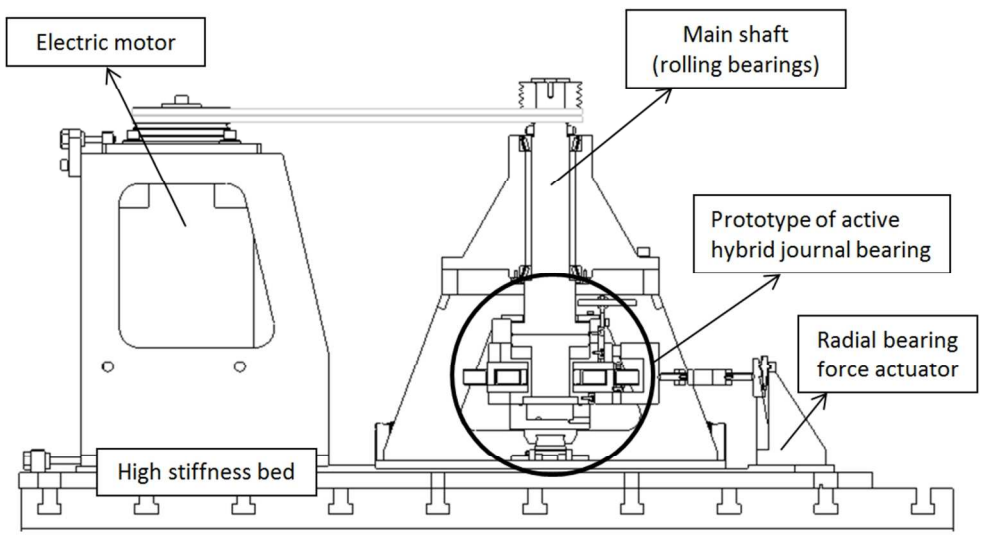
er Review



MR valves picture with description of parts
[insert figure 13]
147x80mm (300 x 300 DPI)

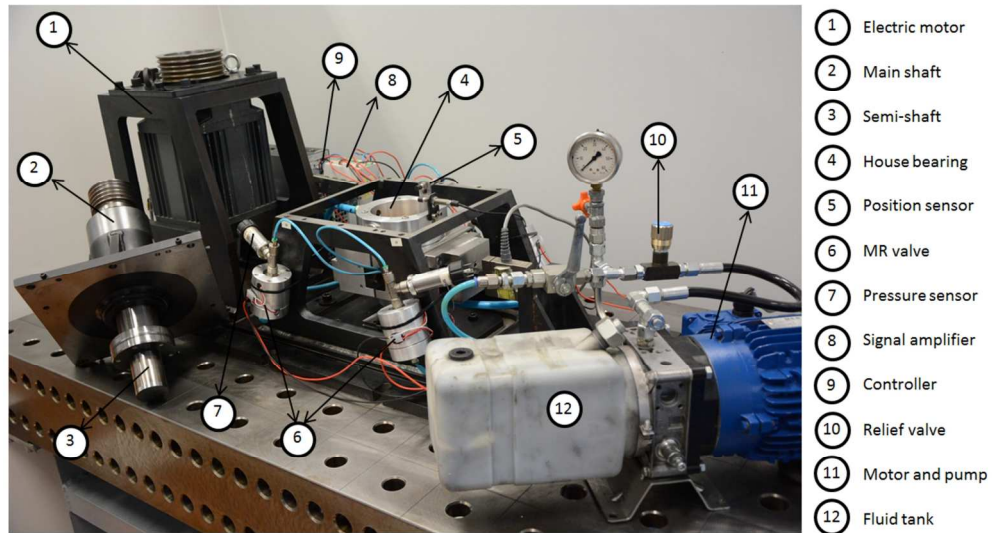
er Review

1
2
3
4
5
6
7
8
9
10
11
12
13
14
15
16
17
18
19
20
21
22
23
24
25
26
27
28
29
30
31
32
33
34
35
36
37
38
39
40
41
42
43
44
45
46
47
48
49
50
51
52
53
54
55
56
57
58
59
60



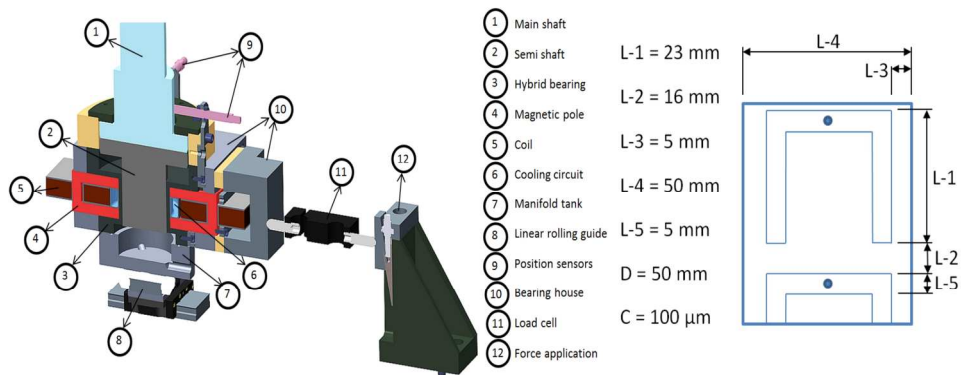
Sketch of hybrid journal bearing test bench and prototype
[insert figure 14]
166x91mm (300 x 300 DPI)

er Review



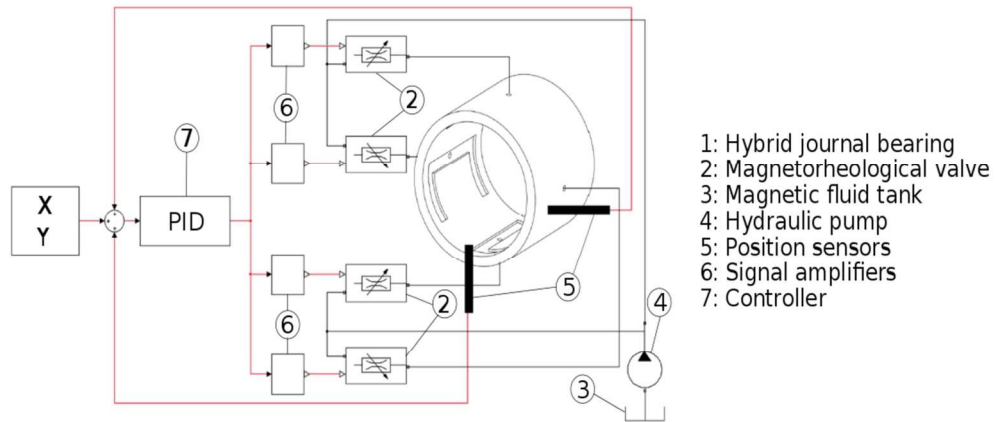
Hybrid journal bearing test bench, overall view
[insert figure 15]
180x99mm (300 x 300 DPI)

1
2
3
4
5
6
7
8
9
10
11
12
13
14
15
16
17
18
19
20
21
22
23
24
25
26
27
28
29
30
31
32
33
34
35
36
37
38
39
40
41
42
43
44
45
46
47
48
49
50
51
52
53
54
55
56
57
58
59
60



Hybrid journal bearing prototype, bearing house section view and dimensions
[insert figure 16]
221x86mm (300 x 300 DPI)

Peer Review

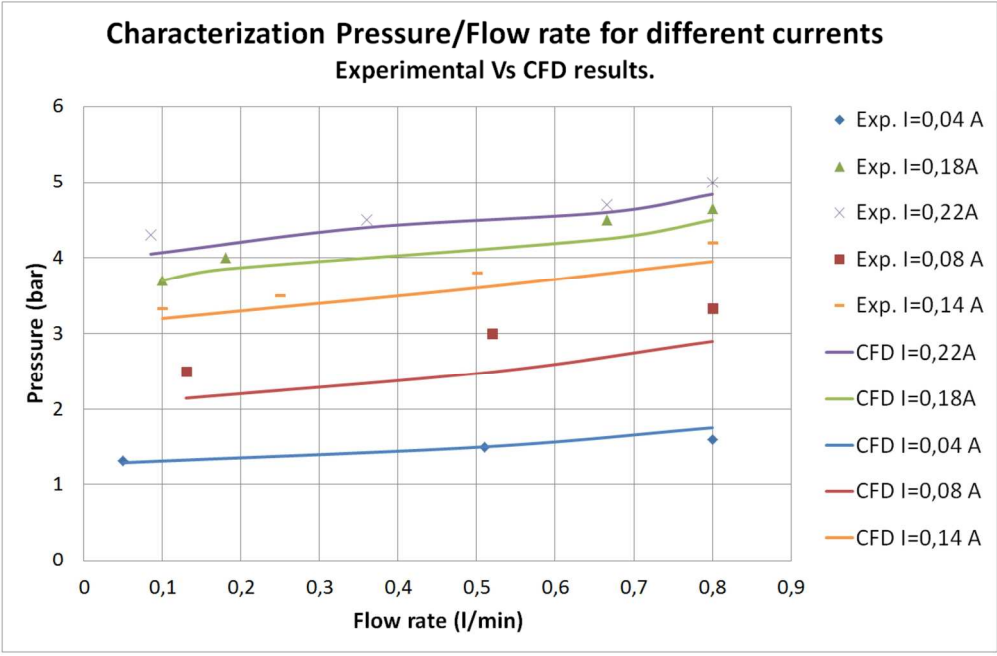


23 Active hybrid journal bearings hydraulic circuit and control
24 [insert figure 17]
25 138x64mm (300 x 300 DPI)

Peer Review

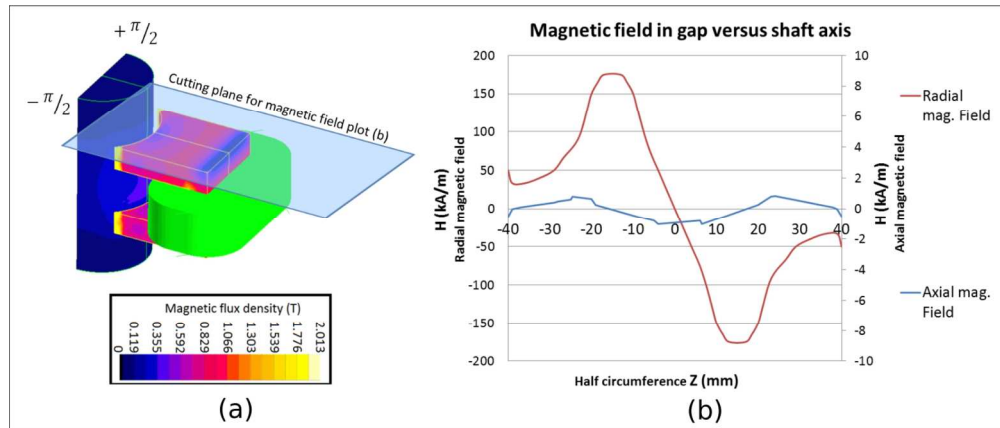
26
27
28
29
30
31
32
33
34
35
36
37
38
39
40
41
42
43
44
45
46
47
48
49
50
51
52
53
54
55
56
57
58
59
60

1
2
3
4
5
6
7
8
9
10
11
12
13
14
15
16
17
18
19
20
21
22
23
24
25
26
27
28
29
30
31
32
33
34
35
36
37
38
39
40
41
42
43
44
45
46
47
48
49
50
51
52
53
54
55
56
57
58
59
60



Experimental and theoretical results in the MR valve for active bearing
[insert figure 18]
231x152mm (300 x 300 DPI)

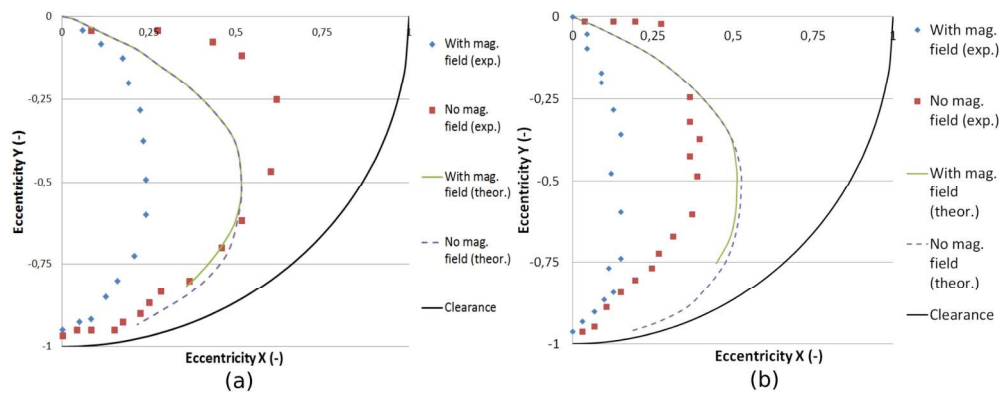
Review



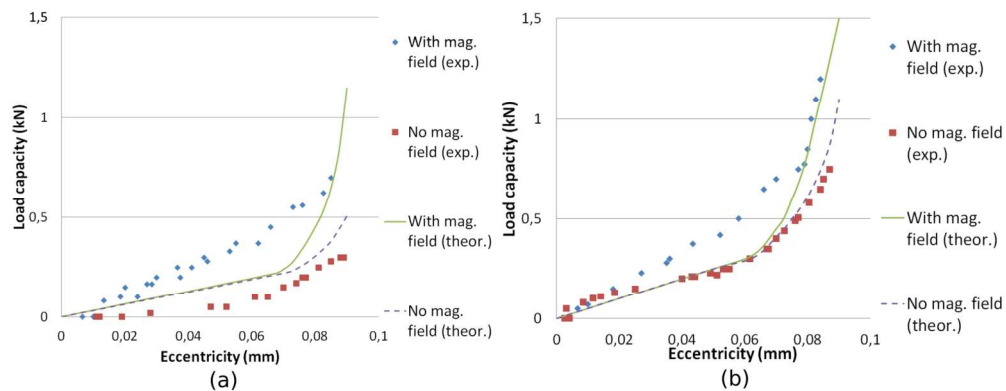
Magnetic field in the hybrid bearing (a), and field strength in the gap (b) for cutting plane defined by (b), half cylinder

[insert figure 19]
190x80mm (300 x 300 DPI)

1
2
3
4
5
6
7
8
9
10
11
12
13
14
15
16
17
18
19
20
21
22
23
24
25
26
27
28
29
30
31
32
33
34
35
36
37
38
39
40
41
42
43
44
45
46
47
48
49
50
51
52
53
54
55
56
57
58
59
60

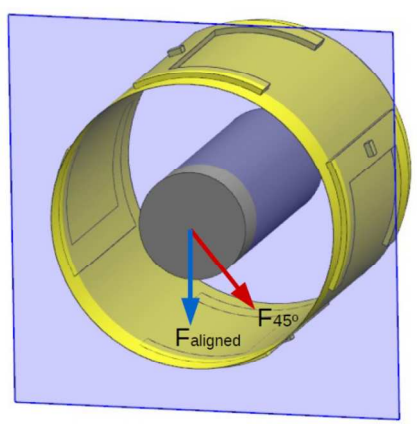


Hybrid bearing, shaft eccentricity path for 50rpm (a) and 200rpm (b)
[insert figure 20]
226x92mm (300 x 300 DPI)

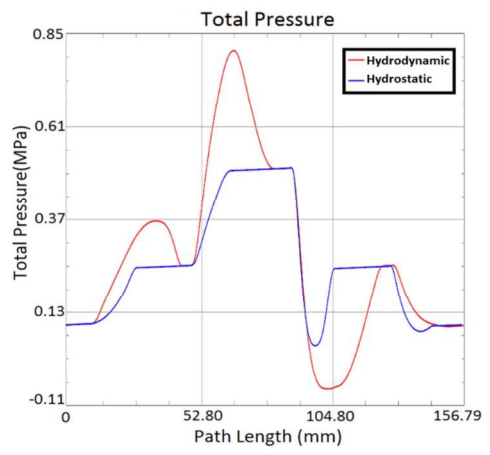


Hybrid journal bearing, load capacity for 50rpm (a) and 200rpm (b)
[insert figure 21]
214x82mm (300 x 300 DPI)

1
2
3
4
5
6
7
8
9
10
11
12
13
14
15
16
17
18
19
20
21
22
23
24
25
26
27
28
29
30
31
32
33
34
35
36
37
38
39
40
41
42
43
44
45
46
47
48
49
50
51
52
53
54
55
56
57
58
59
60



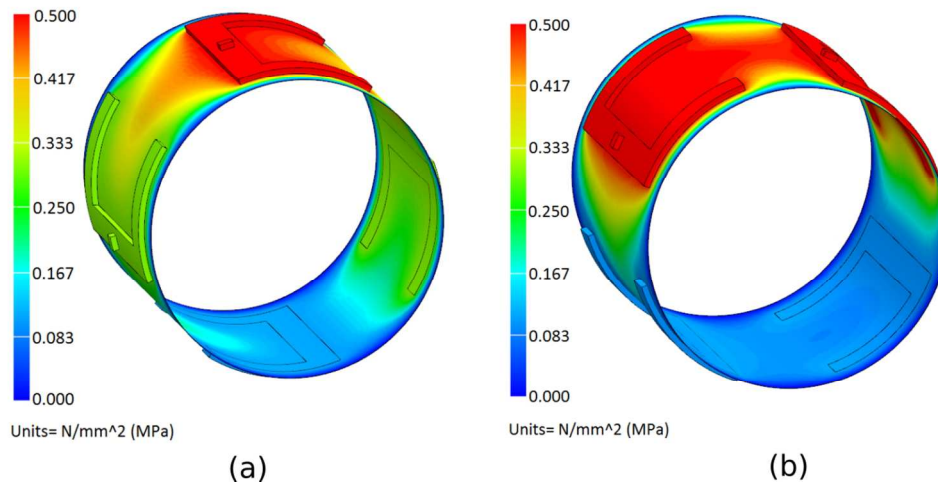
(a)



(b)

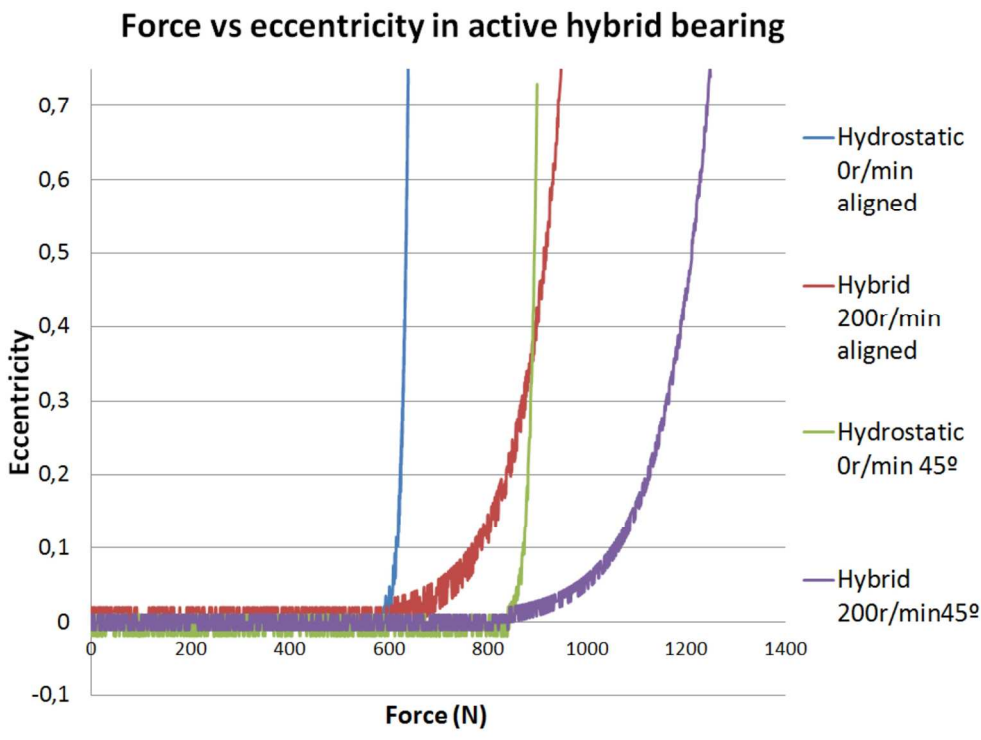
Hybrid bearing, direction of the applied load (a), pressure graph with or without rotational velocity (b)
 [insert figure 22]
 188x90mm (300 x 300 DPI)

Peer Review



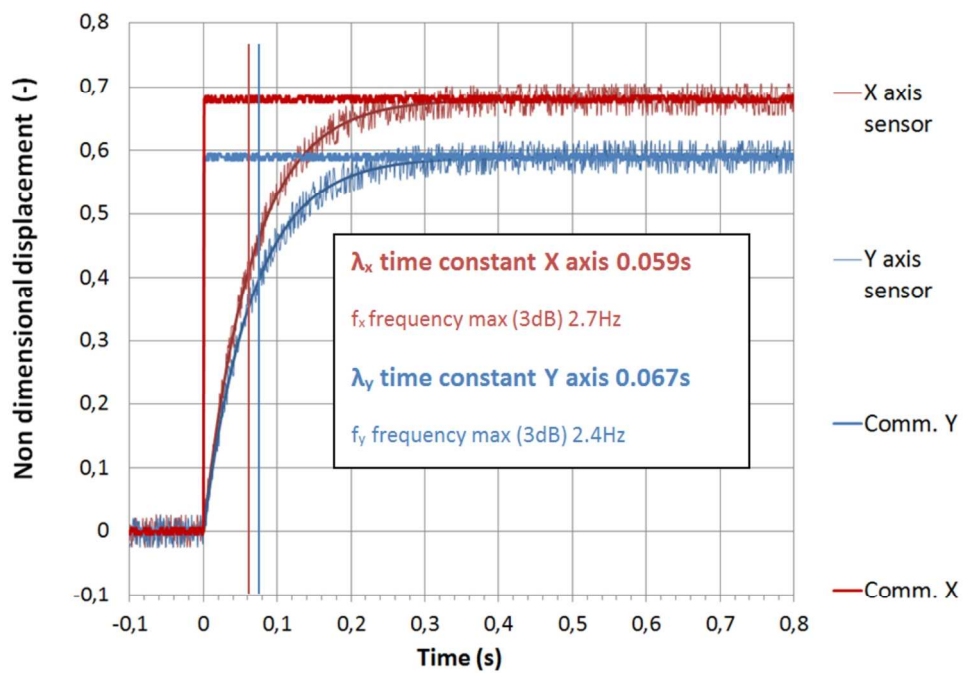
Pressure distribution in the hybrid bearing for aligned (a) and 45° oriented
[insert figure 23]
204x103mm (300 x 300 DPI)

1
2
3
4
5
6
7
8
9
10
11
12
13
14
15
16
17
18
19
20
21
22
23
24
25
26
27
28
29
30
31
32
33
34
35
36
37
38
39
40
41
42
43
44
45
46
47
48
49
50
51
52
53
54
55
56
57
58
59
60



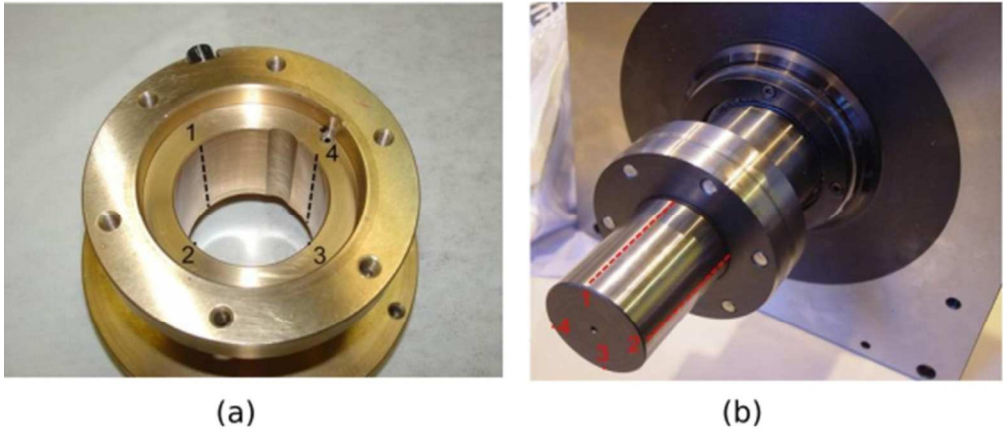
Experimental results of active hybrid bearing under load, stationary values
[insert figure 24]
198x147mm (300 x 300 DPI)

Review



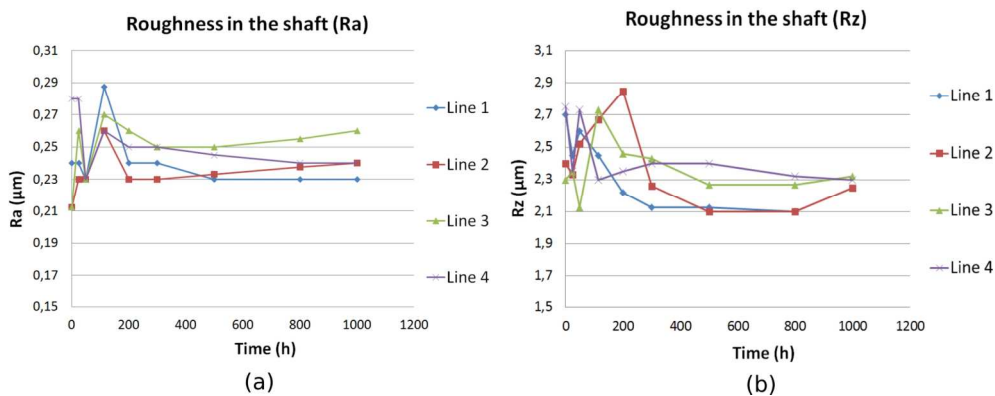
Experimental results of time response in active hybrid bearing
[insert figure 25]
184x129mm (300 x 300 DPI)

1
2
3
4
5
6
7
8
9
10
11
12
13
14
15
16
17
18
19
20
21
22
23
24
25
26
27
28
29
30
31
32
33
34
35
36
37
38
39
40
41
42
43
44
45
46
47
48
49
50
51
52
53
54
55
56
57
58
59
60



(a) (b)
Wear and roughness measuring zones, a) bearing and b) shaft
[insert figure 26]
72x30mm (300 x 300 DPI)

Peer Review



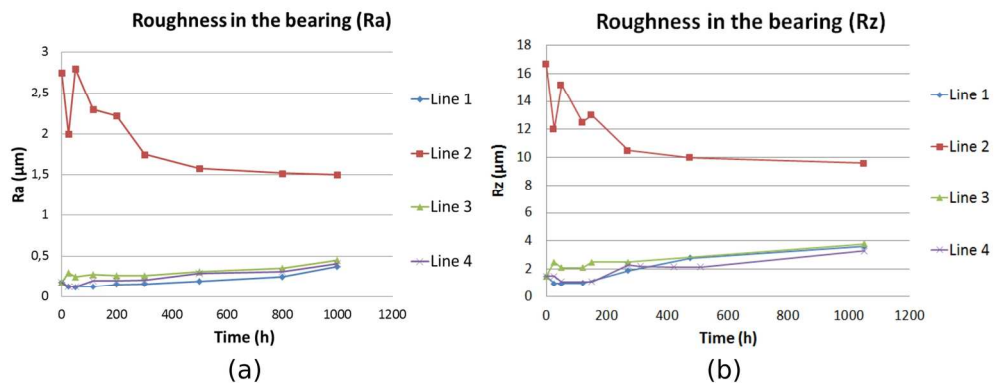
Roughness values in the shaft, a) averaged roughness (Ra), and b) maximum roughness (Rz)

[insert figure 27]

210x83mm (300 x 300 DPI)

Peer Review

1
2
3
4
5
6
7
8
9
10
11
12
13
14
15
16
17
18
19
20
21
22
23
24
25
26
27
28
29
30
31
32
33
34
35
36
37
38
39
40
41
42
43
44
45
46
47
48
49
50
51
52
53
54
55
56
57
58
59
60



Roughness values in the bearing, a) averaged roughness (Ra), and b) maximum roughness (Rz)
[insert figure 28]
178x68mm (300 x 300 DPI)

Peer Review